arXiv:cond-mat/0701062v2 [cond-mat.soft] 31 May 2007

Area constrained SOS Models of Interfaces.

by
J. Stecki

Department III, Institute of Physical Chemistry,
Polish Academy of Sciences,
ul. Kasprzaka 44/52, 01-224 Warszawa, Poland

September 24, 2013

Abstract

The solid-on solid (SOS) model in two dimensions ($d = 2$) is now solved under the constraint of constant energy and then under the new constraint of constant total area. From the combinatorial factors $g(E; L, M)$, the new ensemble is constructed with its free energy $F(A_{tot}, T)$ of a membrane of constant (onedimensional) area A_{tot}. The entropy per column $Y = (1/L) \log g(E; L, M)$ of rectangular $L \times M$ strips reduces to a common curve in reduced variables. Definitions of the "area" and of the interfacial tension, are compared or discussed. Analytical calculations are supported with numerical ones and vice versa. Overall the constraint reduces the ratio of A_{tot} to the projected area L, as compared with canonical calculation, strongly at high temperatures.

I. Introduction

The solid-on-solid (SOS) model originated very long time ago in connection with crystal surfaces and crystal growth; its first extensive description is found in the classical paper of Burton, Cabrera, and Frank[1]. It was later realized that the model of irregularities of a crystal face could be fashioned into a theory of morphology and also of fluctuations of surfaces. Then it was discovered that the SOS model of equilibrium surface could be solved exactly in two dimensions, *i.e.* for a one-dimensional interface, by the method of transfer matrix [2-7]. There are reviews available[8-10]. The solution could be applied to free energy calculations and to the theory of capillary waves[7,11,12] of interfaces.

Here we apply the SOS model to the difficult problem of membrane fluctuations. All interfaces and all membranes as well, undergo shape fluctuations. These necessarily result from thermal motion and are intertwined with all thermal fluctuations. However, there are important distinctions between interfaces and membranes. An interface is an open system, also open with respect to particle exchange. A flat liquid surface increases its surface area and takes a wavy form by inducing the diffusion of molecules from either bulk phase. Similarly a crystal surface is formed and reformed by processes of evaporation - by particle exchange with the surroundings.

In fluctuating membranes such diffusion does not occur or is very rare. Commonly membranes and bilayers are formed by self-assembling surfactant (amphiphilic) molecules and embedded in a liquid solvent. Although in principle the molecules forming a bilayer are soluble to some extent in the liquid solvent, in reality their concentration is exceedingly low. It is hardly possible for a bilayer or a membrane to absorb or release molecules in the process of locally changing its shape; consequently the shape fluctuations (also long-wavelength fluctuations, such as capillary waves) take place *under the constraint* of a constant particle number N_s forming the sheet of surfactant. This constraint translates to a constraint of constant membrane area.

Such considerations will make distinction between the true area and the "projected area". The exact and formal results provided so far by the Gibbs statistical mechanics, always refer to the area defined in terms of the geometry of the macroscopic volume V enclosing the system under consideration. For example in d=3 the volume may be a parallelepiped and the area its $x-y$ edge. A constant-volume increment δF of the free

energy F provides the interfacial tension γ through

$$\delta F = \gamma \delta A \ . \tag{1.1}$$

A is often called the "projected area", to emphasize that, because of the undulations of the interface, its "true area" is larger and, when projected onto the edge of the box, produces A. The "true interface area" is something the external world does not have control of; contrariwise, the projected area A is under the control of external forces just as the volume, temperature, or overall density is. Thus (1.1) defines γ in terms of a measurable quantity A. Such reasoning clearly applies to an interface; we examine the other case of a membrane with a constant intrinsic area.

These observations prompted us to consider a new set of SOS models with constraints. In this paper we limit ourselves to one-dimensional string embedded in two dimensions, *i.e.* to a model which is exactly soluble[2-7] albeit without constaints.

We solve below (for the first time) the microcanonical *i.e.* constant-energy version of the SOS model which we use to obtain the combinatorial factors; these are used to construct the new ensemble of constant interface length. Therefore we proceed via exact enumeration.

In Section II the SOS model is defined and solved; this provides the combinatorial factor $g(E; L, M)$ - the basic building block for subsequent calculations.

These results/calculations have many ramifications, some of which are reported in Section II and in the Appendix because of their novelty and possible usefulness.

In Section III the definitions of the total area are compared and then the relation between total area A_{tot} and the projected area L is compared for the unconstrained calculation and for the new calculations under the constraint of a given constant A_{tot}. Also, the derivative of the free energy with respect to either area (defining the tension γ) is calculated and discussed.

Finally Section IV is the summary and brief discussion.

II. The Solid-On-Solid Model and its Solution.

In the two-dimensional Solid-on-Solid (SOS) model[1-9] a one-dimensional interface is drawn along a strip of a square lattice as illustrated in Fig.1. The interface is reduced to a one-dimensional string. The standard $L \times M$ strip is made of L columns of height

M; the interface crosses each column once and only once. A microscopic configuration of the interface is then specified by a collection of heights

$$\{h_j\}, j = 1, L; \quad 1 \leq h_j \leq M. \tag{2.1}$$

Clusters and overhangs are absent. The "vertical" variable is h or z at the horizontal position $x = a_0 j$, $1 \leq j \leq L$ and we take the lattice constant $a_0 = 1$. The "height" is limited to $1 \leq h \leq M$.

In the standard SOS model[2,5,6] the energy of a microscopic configuration is

$$E_{tot} = E_0 + E \tag{2.2}$$

with

$$E_0 = \epsilon_0 L; \quad E = \epsilon A_v. \tag{2.3}$$

In general $\epsilon_0 \neq \epsilon$ and both are positive. E_0 is the energy of a perfectly flat interface.

The total length of the interface is its one-dimensional area; it is a sum of its horizontal part, A_h and its vertical part, A_v.

$$A_{tot} = A_h + A_v = L + A_v \tag{2.4}$$

The first part is the trivial contribution equal to L. The vertical part is the sum of absolute values of the height jumps

$$A_v = \sum_i \Delta_{i,i+1} = \sum_i |h_{i+1} - h_i| \tag{2.5}$$

where

$$\Delta_{i,i+1} \equiv |h_{i+1} - h_i| \ , \tag{2.6}$$

Thus the energy of the strip and of the interface is directly related to the vertical part of the interface area, A_v. This is not essential.

In more general SOS models where

$$E = \epsilon \sum |h_{i+1} - h_i|^n \quad \epsilon > 0 \tag{2.7}$$

e.g. when $n = 2$ in the Gaussian model, the simple proportionality of E and A_v, is lost.

Also, other definitions of the total area, can be given (see Section III) but are numerically close to (2.4).

We define the following partition functions and their associated thermodynamic potentials. For the finite strip L columns long and M rows high, we have

(A) the microcanonical constant-energy ensemble

$$Z(L, M, E) = g(A_v; L, M) \qquad S = k \log Z \tag{2.8}$$

where g is the number of microscopic configurations and S is the entropy. k is the Boltzmann constant, $E = \epsilon A_v$. Given ϵ_0, one can use interchangeably E_0 or L. Given ϵ, one can use interchangeably E or A_v.

(B) The canonical (constant temperature) partition function is

$$Z(T, L, M) = \sum_{A_v \geq 0} g(A_v; L, M) \times \exp^{-\beta E_{tot}} \tag{2.9}$$

$$\beta F = (-) \log Z \tag{2.10}$$

where F is the free energy. This usually is written subtracting the energy of the flat interface $\epsilon_0 L$ as the trivial term, defining

$$Z(T, L, M) = \sum_{A_v \geq 0} g(A_v; L, M) \times \exp^{-\beta E} \tag{2.11}$$

so that $F = -kT \log Z$ is now the free energy of interface deformations. By introducing the quantity $Q = \exp[-\beta\epsilon] \in [0, 1]$ we rewrite (2.11) as

$$Z(T, L, M) = \sum_{A_v \geq 0} g(A_v) \times Q^{A_v} \tag{2.12}$$

emphasizing that Z is the generating function for combinatorial factors g. Here, L being fixed, the total length of the interface A_{tot} is directly given by A_v and conversely. E, A_v, and A_{tot} fluctuate - appropriately for an interface.

Generalizing the partition function for fixed L, we construct now

(C) the new partition function for total interface area. That is, we consider an ensemble of strips with different lengths L (and common height M). Then

$$Z^*(T, A_{tot}; M) = \sum_L \sum_{A_v} g(A_v; L, M) \exp[-\beta E_{tot}] \tag{2.13}$$

with the implied constraint of a given total area, e.g. defined by (2.4) (as $A_{tot} = L + A_v$). Total energy as given by (2.2)-(2.3) takes into account the energy cost of a horizontal step, ϵ_0, besides the energy cost of a vertical step, ϵ. It is convenient to define

$$Q = \exp[-\beta\epsilon] \quad R = \exp[-\beta\epsilon_0], \tag{2.14}$$

whereby $\exp(-\beta E_{tot})$ is written as $Q^{A_v} R^L$. The partition function (2.13) becomes $Z^*(Q, R, A_{tot}; M)$. By allowing different energies for vertical and horizontal steps we can distinguish and treat as different, total lengths that are equal but are made of different proportions of vertical/horizontal steps. Both $Q \in [0, 1]$ and $R \in [0, 1]$. Thus in (2.12) $R = 1$ has been tacitly assumed. The height M can be made infinite[7,8] for fixed L (Section IId). Under certain conditions, infinite M can also be introduced into (2.13). The averages are calculated as usual: $< L >= -(\partial \log Z)/(\partial \log R)$ and $< A_v >= -(\partial \log Z)/(\partial \log Q)$.

To summarize, we consider the following geometries:

(i) L fixed, M fixed and finite,

(ii) L fixed, M infinite,

(iii) L variable, M fixed and finite,

(iv) L variable, M infinite.

The new partition function for (iii) or (iv) with the constraint of given constant total area $A_{tot} = L + A_v$, is calculated in Section IId.

In all cases we need the basic building blocks: the combinatorial factors $g(A_v; L, M)$ which are computed in Section IIa,IIb, and $g(A_v; L, M = \infty)$ in Section IId.

IIa. The Microcanonical Ensemble of Fixed Energy.

To solve the SOS model in $d = 2$ for both M, L finite and given, one introduces the $M \times M$ transfer matrix as follows

$$T(h, h') = Q^{|h-h'|} \tag{2.15}$$

with $Q \equiv \exp[-\epsilon/kT]$. The canonical partition function is expressed as[2]

$$Z = \text{Tr } T^L = \sum_h (T^L)_{h,h} \ . \tag{2.16}$$

If the transfer matrix is diagonalized, as a real symmetric positive definite matrix it admits a representation

$$T_{hk} = \sum_j \phi_j(h)\lambda_j\phi_j(k) \tag{2.17}$$

where λ_j is the j-th eigenvalue, $j = 1, ..., M$ and ϕ_j the corresponding eigenvector of the orthonormal and complete set. Therefore multiplication of T's just raises the power(s) of eigenvalues and

$$Z = \lambda_1^L + \lambda_2^L + \cdots \quad . \tag{2.18}$$

The largest eigenvalue dominates in the limit $L \to \infty$; then for sufficiently large M, $F/(LkT) = -(1/L)\log Z = -\log\lambda_1 = -\log(1+Q) + \log(1-Q)$ reproduces the known result, $\log\tanh\beta\epsilon/2$ [2,7,10,12].

Now we want to select from the set of all configurations only those of given total length $L + A_v$. If L is fixed this is reduced to a constraint of given A_v. The latter is

$$A_v = \Delta_{12} + \Delta_{23} + \cdots + \Delta_{L,1} \ , \tag{2.19}$$

where

$$\Delta_{i,i+1} \equiv |h_{i+1} - h_i| \ , \tag{2.6}$$

The last term in (2.19) is there if one imposes periodic boundary condition $h_{L+1} = h_1$ as we do. The constraint on A_v can be expressed with the aid of a Kronecker delta $\delta^{Kr}(j,n)$ equal to 1 for $j = n$ and to 0 otherwise. Thus

$$Z(T, L, M; A_v) = \sum_{h_1} ... \sum_{h_L} \delta^{Kr}(A_v, \Delta_{12} + ...) \times T_{h_1,h_2}\ T\ T \cdots \quad . \tag{2.20}$$

By using the integral representation

$$\delta^{Kr}(j,n) = \int_{-\pi}^{+\pi} (\frac{dk}{2\pi}) e^{ik(j-n)} \tag{2.21}$$

and taking the integral in front of the sums, we find that to each T-matrix there corresponds a factor $\exp(ik\Delta)$ so defining the new matrix

$$\tau_{h,h'} \equiv T_{h,h'} e^{ik\Delta_{h,h'}} \quad , \tag{2.22}$$

we have the new expression for the constrained partition function

$$Z(T, L, M; A_v) = \int_{-\pi}^{+\pi} (\frac{dk}{2\pi}) e^{-ikA_v} \mathrm{Tr}\ \tau^L \quad . \tag{2.23}$$

This is the expression we evaluate. The matrix τ can be put into the form of the r.h.s. of (2.15); define $\tilde{Q}$ as $\tilde{Q} \equiv Q \exp(ik)$, so that

$$\tau(h,h') = \tilde{Q}^{|h-h'|} \qquad \tilde{Q} \equiv e^{+ik-\beta\epsilon} \quad . \tag{2.24}$$

The complex $\tilde{Q}$ has a real part between -1 and 1 and an imaginary part between -1 and 1. The matrix τ depends parametrically on the wave-vector k, the integration variable, which is real. It reduces to the original T-matrix at $k = 0$, apparently continuously. By using the package "Eispack"[13], in particular its program CG for diagonalization of complex general matrices, we were able to compute Z and log$Z$ from

$$Z(T,L,M;A_v) = \int_{-\pi}^{+\pi} (\frac{dk}{2\pi}) e^{-ikA_v} [\lambda_1(k)^L + \lambda_2(k)^L + \cdots + \lambda_M(k)^L] \; . \tag{2.25}$$

The eigenvalues depend on k. Evaluation was done for $M = 5, 6, 10, 20$ and for $L < 41$; several values of Q were used. It could be done for $M = 30$. For odd A_v the result is exactly nil and this is correct because of the periodic boundary condition at L. For $A_v = 0$, $Z = M$ for all Q. The general form of the result is

$$Z(A_v) = g(A_v) Q^{A_v} \; . \tag{2.26}$$

with g independent of Q. The Kronecker delta picks up the one term of the sum (2.12). By dividing (2.26) by Q^{A_v} we obtain $g(A_v; L, M)$. All numerical results did conform to (2.26); g was obtained accurately for the very largest systems (g must be an integer) and was obtained exactly for all other sizes. Numerically, Q cannot be chosen too small or too close to unity. In actual calculations we have imposed periodic boundary condition $h_{L+1} = h_1$ which not only simplified the calculation but also excluded exotic configurations. For all A_v odd, g is nil.

The combinatorial factor $g(A_v)$ always follows the same pattern starting from $g(0) = M$, going through a maximum near $A_v \sim LM/3$ and then falling down to 0 for $A_v > (M-1)L$. Being the number of microscopic configurations, g very soon reaches horrendously large numbers and for that reason Fig.2 shows an example of $g(A_v)$ for very small M, L. The pattern seen in Fig.2 is general; starting with $g(0) = M$ and after a very rapid increase, g goes through a maximum and falls to a low value, often terminating with a value of 2. Afterwards for all values of A_v the correct value is $g = 0$. This characteristic dependence becomes continuous for large L (and not too

small M) in the following variables: $Y = (1/L)\log(g)$ and $a \equiv A_v/Ln_1$. The quantity $a \equiv A_v/Ln_1$ varies between 0 and 1 , n_1 being equal to $M-1$.

Since the energy is not allowed to fluctuate, the logarithm of the partition function is the thermodynamic potential of the constant-energy microcanonical ensemble

$$S(L, M, E) = k \log g(A_v; L, M) \quad E = \epsilon A_v \tag{2.27}$$

An extension of the numerical results to larger systems, can be based on a simple scaling in reduced variables. We have already introduced the scaled, or reduced area (simply area per site) $a \equiv A_v/L(M-1)$ and we find that $Y = (1/L)\log(g)$ fall on a common curve when plotted against a, for different L at each constant M.

Fig.3 shows how this simple "scaling" works; the shapes are similar enough so that for each M different values of L fall on a common curve. Values of $L < 10$ and of $M < 10$ are too small to be included.

Eq.(2.27) identifies the function Y as entropy per column. Invoking the relation

$$dS/dE = 1/T \tag{2.28}$$

defining the thermodynamic temperature T in the microcanonical ensemble, we may rewrite it as $d\log(g)/dA_v = \beta\epsilon = -\log Q$ with $\beta = 1/kT$. However, as a look at Fig.2 and Fig.3 shows, beyond the maximum in g that interpretation fails (or produces negative temperatures). The original observation is attributed to L.Landau[14]: in systems with energy bounded from above, $T < 0$ is possible. Here is one more such example.

The ordinary canonical partition function is calculated by diagonalizing the real $T-$matrix for given Q, *i.e.* after (2.16-18). But it is also equal to (2.12) . Since all terms are positive, selecting the maximum term leads to $d(\log g)/dA_v - \beta\epsilon = 0$ which can be rewritten to a form like (2.28). Now T is an independent variable, $T > 0$ because $Q \in [0, 1]$, and $E = E(T), S = S(T)$.

IIb. An Independent Algebraic Check.

Turning to the starting point for the solution of the model, (2.15-2.16), we note that for small L the trace can be computed analytically. By multiplying out the T-matrices, we obtain a polynomial in Q:

$$Z = TrT^L = c_0 + c_1 Q + c_2 Q^2 + ... \quad . \tag{2.29}$$

The basic observation is that the power of Q is just the number of energy units, identified in the previous subsection as the vertical part of the total length and denoted by A_v. Z containing the total of all configurations, each term represents the split between different values of A_v. That is , we can identify the coefficients c_j in (2.29) as the combinatorial factors denoted by $g(A_v)$. Thus equation (2.29) is rewritten as

$$Z = \sum_{A_v=0,1,2...} g(A_v) Q^{A_v} \ . \tag{2.12}$$

For example, constructing the 4 by 4 T-matrix (whose first row is $1, Q, Q^2, Q^3$) and multiplying it out to obtain T^6, taking the trace, we obtain for $L = 6, M = 4 \quad Z = 4 + 90x^2 + 510x^4 + 1266x^6 + 1116x^8 + 744x^{10} + 310x^{12} + 42x^{14} + 12x^{16} + 2x^{18}$. Thus $g(A_v = 8) = 1116$ etc. See Fig.2. Such exact enumerations, with the computer-aided algebra, were carried out up to $M = 20$ for L up to 30, providing checks on numerical results obtained via the diagonalization described in previous Subsections.

IIc. The Constraint of Total Area For Given M

From the combinatorial factors in the microcanonical ensemble at given L, M we can construct now the partition function with the constraint of total length A_{tot}. We take the ensemble of strips with different L's (and the same M) and implement the constraint of constant A_{tot} in (2.13); for given M

$$Z^*(T, A_{tot}; M) = \sum_L \sum_{A_v} \delta^{Kr}(L + A_v, A_{tot}) g(A_v; L, M) Q^{A_v} R^L. \tag{2.30}$$

That is, the sum $L + A_v$ is held constant. Maximum value of L is obviously A_{tot} and the mimimum value is 2. To avoid exotic cases, periodic boundary conditions are imposed $h_L = h_1$. The Kronecker delta is replaced by these simple restrictions on the sums.

Note that here we do not calculate the average total area A_{tot} because the procedure is inverted: for *given* fixed total length A_{tot} both L and A_v are allowed to fluctuate and are calculated as averages:

$$\langle L \rangle = d \log Z^* / d \log R \quad \langle A_v \rangle = d \log Z^* / d \log Q \tag{2.31}$$

and $\langle A_v \rangle = A_{tot} - \langle L \rangle$ or conversely. The averages as $f(Q, R, A_{tot})$ were computed and are shown below for special cases such as $u \equiv Q = R$ and $R = 1, Q \in [0, 1]$. In

the first case a string of fixed length is allowed to fluctuate in a neutral environment, where energy of a horizontal step is equal to that of a vertical step and therefore none is preferred; in the second case, only the energy of vertical steps is affecting the choice of configuration.

Interestingly, the conbinatorial factors $g(A_{tot})$ are increasing without bounds, in contrast to the constant L, M case from Section IIa-IIb.

For an ensemble of narrow strips of $M \geq 6$ analytical calculations were done as follows: first traces of T^L were calculated and stored (for L up to 40 and nore) and then sums were formed for all even values of $A_{tot} \in [10, 38]$. From the resulting expression $\beta F, \langle L \rangle, \langle A_v \rangle$ were calculated analytically and used, in part to check the results of numerical computations. A selection of these results is shown in Section III. The results for finite M are also compared with the case $M = \infty$ described below.

IId. The Columnar Strip (M=∞) and its Solution.

From the solution[7] of the eigenvalue problem of T for given L and columns of infinite height[7], $M = \infty$, the eigenvalues are known explicitely

$$\lambda(\nu) = (1 - Q^2)/(1 + Q^2 - 2Q\cos(\nu)) \tag{2.32}$$

where the index $\nu \in [-\pi, +\pi]$ is now continuous. Because of the translational invariance in the "vertical" M direction, actually exploited in solving the transfer matrix[7], we must impose a constant h_1, e.g. $h_1 = 0$ and another fixed value for h_L - which we choose to be equal to h_1. The canonical partition function (2.11) or (2.12) with M infinite then exists. There are some limitations in more general cases ($R \neq 1$ and variable L fixed A_{tot}) - because now the excursions of the interface are limited only by the cost of a vertical step. The flat configuration $h_i = 0$ is the equilibrium configuration for $Q \to 0$.

We need the combinatorial factors $g(A_v; L, M = \infty)$. Following Section IIa, in order to impose the the constraint of fixed A_v we replace $Q = \exp(-\beta\epsilon)$ with $\tilde{Q} \equiv Qe^{ik}$. The solution[7] goes through as explicit calculation shows. The partition function becomes a double integral, replacing (2.25) by

$$Z(Q, A_v; L, M = \infty) = \int_{-\pi}^{+\pi} (\frac{dk}{2\pi}) e^{-ikA_v} \int_{-\pi}^{+\pi} (\frac{d\nu}{2\pi}) \lambda(\nu)^L \ . \tag{2.33}$$

Numerical evaluation is now simpler as the diagonalization step is not needed - we have the explicit expression (2.32) for the eigenvalues. For A_v and L integers, we obtain again Z in the form (2.26) *i.e.* $Z = g \times Q^{A_v}$, where again $g(A_v)$ comes out an integer. Again $\log g$ has the interpretation of entropy S/k.

In an analytic calculation, all $g(A_v; L)$ result as polynomials in A_v. There is a striking simplification which occurs for $M = \infty$; $g(A_v; L)$ are polynomials with highest power equal to $L - 2$. For example $g(x; L = 4) = 2 + (2/5)x^2$ (for all $x > 0$), $g(x; L = 6) = 2 + (35/8)x^2 + (21/32)x^4$ etc. $(x \equiv A_v)$. Knowing these polynomials we can make computations with *any value* of A_v. A few examples are given in the Appendix.

The exact results for $g(A_v; L, M = \infty)$ are used now to construct an ensemble of columnar strips of infinite heights M and variable L. At given A_{tot}, maximum value of L is A_{tot}, and the mimimum value is 2. Minimum value of A_v is zero; there is no upper bound other than $A_{tot} - L$. To avoid exotic cases and to ensure the existence of Z, again $h_L = h_1 = 0$ for each L. We show here, in Section III, explicit calculations for these two cases: $Q = R \to u$ and $R = 1, Q \in [0, 1]$.

III. Numerical Results and the Comparison of Areas and Free Energies.

In this section we show a restricted selection of results for the two most important quantities: the vertical area A_v related to the energy and the total area of the interface. We also consider the derivative of the free energy F with respect to area, all other variables being kept constant; this is interpreted as the interfacial tension γ. Hence

$$\beta\gamma = (\partial(\beta F)/\partial A)_T \tag{3.1}$$

The area A can be the projected area L, the total area imposed in the ensemble of all L's, or the average total area defined as $\langle A_{tot}\rangle \equiv L + \langle A_v\rangle$. All results are given for $R = 1, Q \in [0, 1]$ (cf.(2.13)-(2.15)). The other interesting case, $R = Q \in [0, 1]$, turns out to be a degenerate temperature-independent one, in which the interface wiggles randomly in an energetically neutral environment. These results are also reached in the limit $Q \to 1^-$ at constant $R = 1$.

First, however, we compare 3 different definitions of the area, or, rather, two definitions, A_v and A_{sq}, and one approximation, A'. Our definition of the total area as $A_{tot} = L + A_v$ corresponds to the length of the thick line in Fig.1; L is the sum of "horizontal" steps, and A_v is the sum of "vertical" steps, $\Delta_{i,i+1}$ (cf. (2.5-6). The usual

definition would draw a line through h_i and h_{i+1}; this approach produces

$$A_{sq} \equiv \sum [-1 + \sqrt{1 + \Delta_{i,i+1}}]. \tag{3.2}$$

where L is subtracted. Expansion of the square root gives the first term, which is the common approximation,

$$A' \equiv \sum (1/2)\Delta^2_{i,i+1}. \tag{3.3}$$

Definitions A_v and A_{sq} produce always very close results, A_v always slightly larger. Fig.4 shows all three areas calculated in the canonical ensemble, plotted against Q. A' is a very bad approximation, grossly exaggerating A_{sq} except when both are very small; this happens here at small Q. We have found earlier in another context[15] the same pattern, with the commonly used approximation for the area, like (3.3), grossly overestimating the true area, except in the limit $\Delta A \to 0$.

Figure 4 also includes the microcanonical results *i.e.* the curve of A_v as independent variable against $Q = \exp(-\langle \beta\epsilon \rangle)$ with the inverse temperature computed acccording to (2.28) with (2.27); even for the small value of M the differences are negligible and invisible on the scale of the plot. This is a useful check; the agreement between the canonical and microcanonical ensembles can only become better for larger L and M and it does. In conclusion, we use $A_v + L$ as a measure of area, include canonical averages, and do not quote microcanonical averages.

Fig.5 illustrates the results for the new ensemble of variable L and constant A_{tot}. Three values $A_{tot} = 10, 20, 30$ were chosen. Since $A_{\rm sq}$ and A_v are so close, only $\langle A_v \rangle$ is plotted. The case $M = \infty$ (section IId) is shown with lines; at the infinite temperature $\langle A_v \rangle$ reaches 4.2, 9.2, and 14.2 for $A_{tot} = 10, 20, 30$, respectively. Interestingly, squeezing the membrane with a small $M = 6$ does not change $\langle A_v \rangle$ much; these averages are shown with stars, crosses, and plus signs, and reach 4.0, 8.6, and 13.0. Unconstrained averages calculated in the canonical ensemble produce plots of another shape and much larger values at high temperatures; $\langle A_v \rangle$ for $M = \infty$ diverges. For fixed A_{tot} it does not.

We choose the inverse temperature as the ordinate for the plot because of the quasi-linearity at high temperatures of the data with fixed A_{tot}. As can be seen clearly, fixing A_{tot} limits the vertical excursions of the interface considerably and - somewhat suprisingly - in a similar fashion for small $M = 6$ and for $M = \infty$. At low temperatures i.e. at vanishing Q and large $\beta\epsilon$ all calculations produce $\langle A_v \rangle \to 0$.

At $Q = 1$ *i.e.* $\beta\epsilon = 0$, $\langle L \rangle$ is at 55-57 percent of A_{tot}, practically in all calculations we have done so far for the new ensemble. The limit corresponds to the fluctuation of the interface in the neutral environment where horizontal or vertical steps carry the same cost in energy, now vanishing in the limit $Q \to 1, \beta\epsilon \to 0$.

The divergence of the canonical average for $M = \infty$ (full line in Fig.5) can be understood as follows. If $M = \infty$ and L is fixed whereas A_v and A_{tot} are free to fluctuate and take an average value, it is only the energy cost expressed in the value of Q which limits the excursions of the interface and therefore the number of realized configurations thus the partition function. When Q ceases to operate, the partition function and the averages, diverge. This does not happen when a fixed A_{tot} is imposed.

All partition functions are converted to free energies and all free energies depend on an area as the independent extensive variable. The definition (3.1) of the interfacial tension γ, is now applied to $\beta F(A_{tot}; T)$. In Fig.6 the derivative (3.1) w.r.to A_{tot} is plotted against Q. For $M = \infty$ or $M = 6$ in the ensemble of all L, the data points show mild near linear variation with Q.

For comparison, the canonical free energy per column $\beta F(Q; L, M)/L$ from the largest eigenvalue, is $-\log[(1+Q)/(1-Q)]$ and is plotted as the dot-dash line. All eigenvalues for $M = 6$ produce the near-linear full line.

Whether the derivative (3.1) applied to $F(A_{tot}, T)$ can be interpreted as an "interfacial tension", is perhaps debatable. Still the derivative can be calculated and compared with other derivatives of the free energy with respect to other areas.

IV. Summary and Discussion.

As recalled in the introduction membranes keep their area constant, notwithstanding shape fluctuations. Planar interfaces are also twodimensional sheets embedded in three dimensions, but are open to particle exchange with the surroundings and their proper or intrinsic area varies. Hence the theory of fluctuating interfaces must be suitably modified to apply to membranes. We examine this modification by choosing an existing simple and soluble model, namely the SOS model in two dimensions, for which exact enumerations were practical.

By starting from the available results, we introduced the constraint of constant interface area; first simply into the $L \times M$ strip and then constructing a new *ensemble of all projected areas.*

The partition functions, free energies, and the ensemble averages all were built on the microcanonical combinatorial factors $g(A_v; L, M)$. Their calculation was essential. These were obtained by several means described in Section II. Of the several calculational schemes, the ensemble of all lengths L at infinite height M under the constraint of a given total area A_{tot} produced $\langle A_v \rangle$ and $\langle L \rangle$. The latter has an interpretation of the average projected area. Practically in all calculations, the ratio $\langle L \rangle / A_{tot}$ approached 55 percent in the limit of high temperatures ($Q \to 1, \beta\epsilon \to 0$).

We also calculated the derivative of the free energy $F(A_{tot}, T)$ with respect to A_{tot}. This may be considered an analogue of the interfacial tension γ, now defined with respect to A_{tot}. When compared with other calculations of similar derivatives, the new derivative was the smallest in the absolute value and did not diverge in the limit of infinite temperature. This was illustrated by Fig.6.

The mathematical procedures involved some particular features; their description may be useful. First, we used a diagonalization of a complex matrix τ which was symmetric but not unitary. This was followed by numerical integration. The final result had to be an integer. The correcteness of the diagonalization procedure was verified by agreement with the exact algebraic calculations. The exact enumerations (for the case of infinite M) were also spot-checked by the generating functions for "partially directed" random walks, obtained by slightly modifying the generating functions given by Privman and Svrakic[18]; but introduction of constraints was, as often is the case, not any more practical.

Extension to two-dimensional membranes embedded in $d = 3$ is not impossible though difficult. A good candidate[17] is the Gaussian SOS model on a square lattice with each site endowed with a continuous height variable h_i; it is readily soluble without constraints and for various boundaries. The prediction is that the constraint will damp the fluctuations in a way similar to the damping seen here.

Finally, it is probably all too obvious that our aim was not to develop further the Solid-on-Solid model but rather to use it to examine the differences between membranes and interfaces. Thus we have not pushed the calculations in order to go to highest possible orders of calculation . The trends are already visible.

Acknowledgements.

The author has greatly benefitted in the past from discussions with J.S.Rowlinson

FRS (Oxford), R.Evans FRS (Bristol), and B. Widom (Cornell).

Appendix.

Combinatorial Factors g for Infinite M.

It is a rare and desirable event if combinatorial factors can be generated by polynomials. We list the first few combinatorial factors $g(x)$ for L =2, 4, 6, 8, 10. These were calculated and are available for L up to 30. These polynomials are valid for any value of $x \equiv A_v > 0$. For $x = A_v = 0$, $g = 1$ for any L. Some exact algebraic calculations were done in part with the aid of an old version of "Mathematica"[16]. See Section IIc for notation and further details.

L= 2 $g = 2$

L= 4 $g = 2 + (5/2)x^2$

L= 6 $g = 2 + (35/8)x^2 + (21/32)x^4$

L= 8 $g = 2 + (707/120)x^2 + (77/48)x^4 + (143/1920)x^6$

L=10 $g = 2 + (14465x^2)/2016 + (4147x^4)/1536 + (715x^6)/3072 + (2431x^8)/516096$ ...

References.

1. W. K. Burton, N. Cabrera, and F. C. Frank, Phil. Trans. Roy. Soc.(London) **243**, No.866,299-358 (1951); Nature **163**,398 (1949).
2. J. M. J. van Leeuwen and H. J. Hilhorst, Physica **A107**, 319 (1981).
3. S. T.Chui and J. D. Weeks, Phys. Rev. B **23**, 2438 (1981).
4. T. W. Burkhardt, J. Phys. **A14**, L83 (1981).
5. D. M. Kroll and R. Lipowsky, Phys. Rev. B **28**, 5273 (1983).
6. A. Ciach, Phys. Rev. B **34**, 1932 (1986).
7. A. Kooiman, J.M.J. van Leeuwen, R.K.P.Zia, Physica **A170**, 124 (1990).
8. D. B. Abraham, in *"Phase Transition and Critical Phenomena"*, (C. Domb and J. L. Lebowitz, Eds.), Vol.10, Academic Press, London (1986).
9. V. Privman, Chapter 1 in *"Finite Size Scaling and Numerical Simulation"*, (Singapore, 1990) where further references can be found.
10. J. Dudowicz and J. Stecki, in *"Fluid Interfacial phenomena"*, (C. A. Croxton, Ed.)

J. Wiley 1986, p. 637ff.

11. A. Ciach, J. Dudowicz, and J. Stecki, Phys. Rev. Lett. **56**, 1482 (1986).
12. A. Maciolek and J. Stecki, Phys. Rev. B **54**, 1128 (1996).
13. Eispack - Fortran package maintained by Argonne Natl. Laboratory, version 1983.
14. L. D. Landau and L. Lifshitz, *"Statistical Physics"* (Pergamon, Oxford 1980).
15. J. Stecki, J. Chem. Phys. **114**, 7574(2001), cf.eq.(5.4) ff.
16. Mathematica - a software package (ver.2.2) by Wolfram Research, Inc. (1994).
17. J. Stecki, in preparation.
18. V. Privman and N. M. Svrakic, *"Directed Models of Polymers, Interfaces, and Clusters"*, Springer-Verlag (Lecture Notes in Physics No.338), Berlin 1989.

Figure Captions

Figure 1

The solid-on-solid (SOS) interface in $d = 2$. The strip is M sites wide in the "vertical" direction and L sites long in the "horizontal" x direction. The interface is of length $A = L + A_v$.

Figure 2

An example of the number g of configurations of the interface plotted against the interfacial area A_v at given size of the strip with L=6,M=4. The numbers (different from zero) are: 4, 90, 510, 1266, 1116, 744, 310, 42, 12, 2, for areas A_v 0,2,4,6,8,...,18, respectively.

Figure 3

The "scaling" curve of the microcanonical combinatorial factor $g = g(A_v)$ at fixed L, M. The function $Y = (1/L)\log(g)$ is plotted against $a = A_v/L(M-1)$ for $M = 6, 10, 20$, and $L = 10, 20, 30$. Smaller values of L deviate from the common curve. The maxima extrapolated to $1/L \to 0$ with polynomials in $1/L$ were 1.77702, 2.28587, and 2.97979 for $M = 6, 10, 20$, respectively. Extrapolation to $1/M \to 0$ was inconclusive.

Figure 4

Three areas: A_v/L, A_{sq}/L, and A'/L vs. Q calculated in the canonical ensemble (see text) are compared. Full line terminating at 5.8198 - A_{sq}/L; bold-dashed line hitting 33.25 - A'/L; fine-dashed line hitting 6.6500 - A_v. Plus signs - microcanonical A_v reaching 6.564 at $Q = 1$. $L = 30$,$M = 20$. A_v/L was independent of L and weakly depending on M provided $M \geq 10$.

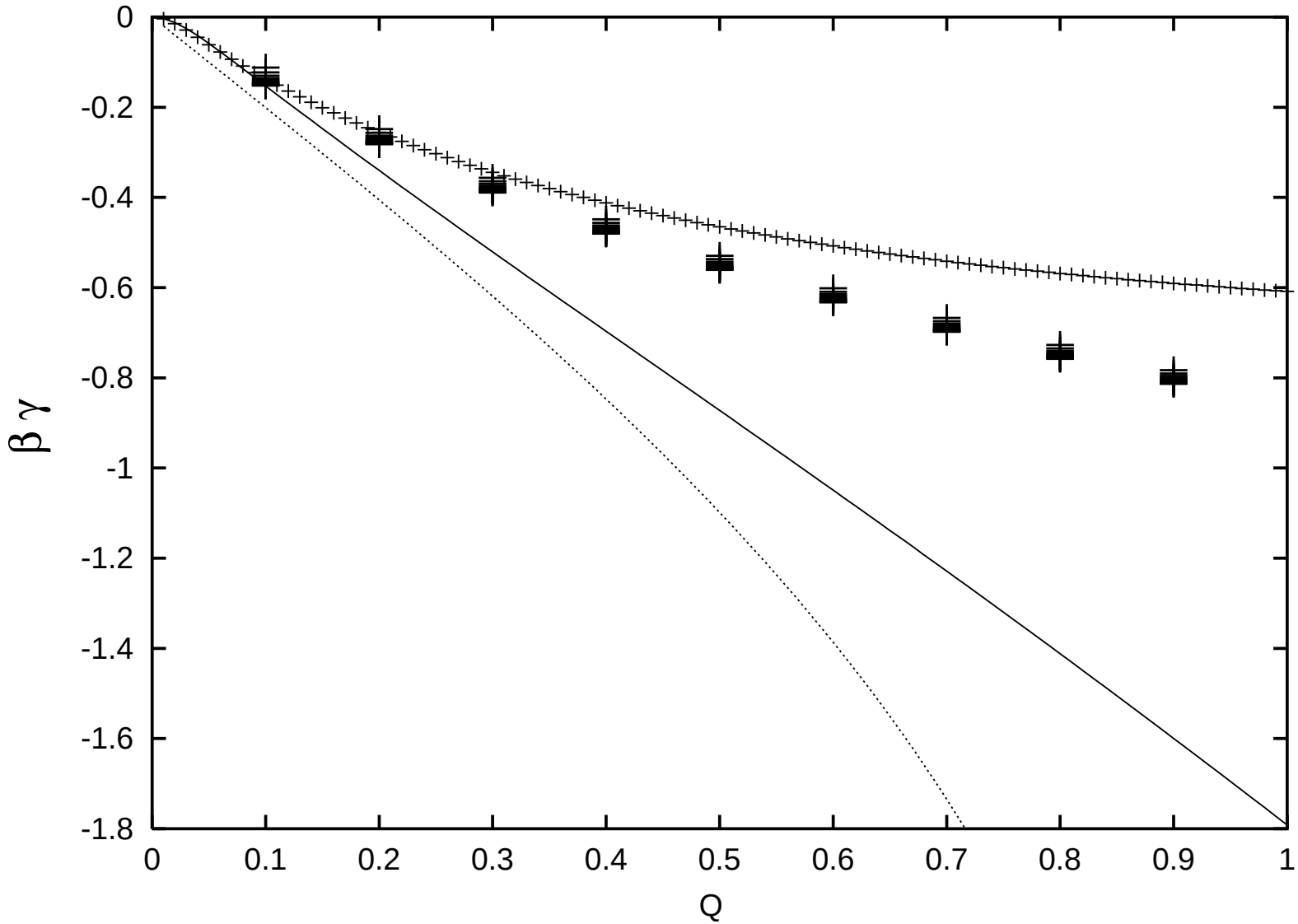
Figure 5

Average $\langle A_v \rangle$ vs. $\beta\epsilon = \epsilon/kT = -\log Q$ for fixed $A_{tot} = 10, 20, 30$ in the ensemble of all L. Fixed $M = 6$ shown with points (stars, crosses, plus signs, respectively); $M = \infty$ shown with lines (fine-dashed, dashed, full, respectively). Unconstrained canonical averages $\langle A_v \rangle$ for constant L, M are ($M = 6, L = 10, 20, 30$, - dotted lines; ditto $M = \infty, L = 10$, - full line) . For $\beta\epsilon = 0$, data shown with points hit 4.00, 8.564, 12.980, respectively; data for $M = \infty$ shown with lines, hit 4.205, 9.209, and 14.213, respectively. The dotted lines (canonical $\langle A_v \rangle$ for $M = 6$) hit 19.444, 38.888, 58.333 for L=10,20,30, respectively. $R = 1, Q \in [0, 1]$ in all cases.

Figure 6

Free energy derivatives w.r.to the total area $(\partial\beta F/\partial A_{tot})_Q$, plotted against Q. The new ensemble of all L and $M = 6$ - small plus signs, ditto $M = \infty$ -large plus signs. For comparison the derivatives w.r.to the projected area L, in canonical ensemble $M = 6$ - full line, $M, L \to \infty$ - dash-dot line, are plotted.

the end of text. Figures are as 6 *.eps files


0
-0.2
-0.4
-0.6
-0.8
-1
-1.2
-1.4
-1.6
-1.8
β γ
0
0.1
0.2
0.3
0.4
0.5
0.6
0.7
0.8
0.9
1
Q